Theor Chem Acc (2000) 104:296–301
DOI 10.1007/s002140000120

Theoretical
Chemistry Accounts

Regular article

Recombination of silicon ions by electron capture from atomic hydrogen and helium

M. C. Bacchus-Montabonel

Laboratoire de Spectrométrie Ionique et Moléculaire (UMR 5579), CNRS et Université Lyon I,
43 Bd du 11 Novembre 1918, 69622 Villeurbanne Cedex, France

Received: 14 September 1999 / Accepted: 3 February 2000 / Published online: 2 May 2000

Abstract. Ab initio potential-energy curves and coupling matrix elements of the Σ and Π molecular states involved in the collision of the Si^{2+}, Si^{3+} and Si^{4+} multicharged ions on atomic hydrogen and helium have been determined by means of configuration interaction methods. The total and partial electron capture cross sections have been determined using a semiclassical or a quantal approach in the 0.002–0.1 au velocity range. A detailed comparison with very recent theoretical and experimental rate coefficient results is made.

Key words: Electron capture – Silicon ions

1 Introduction

The charge-transfer recombination with atomic hydrogen and helium is an important process in astrophysical plasmas for many low charged ions whose emission lines are used to provide direct information on the ionization structure of astronomical objects. Great interest has been paid very recently to silicon ions [1–15], with the experiments of Fang and Kwong [16, 17] providing some of the first experimental data on charge-transfer rate coefficients at low temperatures. Silicon is found in a variety of astronomical plasmas and several important charge-transfer processes may be suggested. In particular the charge-exchange recombination of Si^{2+} and Si^{3+} may lead directly to the formation of a ground-state ion and thus may induce rapid ionization via the inverse charge-transfer process. Such reactions are critical in determining the fractional abundances of silicon ions. We have considered the three main reactions

$$Si^{2+}(3s^2)^1S + H(1s)^2S \rightarrow Si^{+}(3s^2 3p)^2P^0 + H^{+} \quad (1)$$

$$Si^{3+}(3s)^2S + He(1s^2)^1S \rightarrow Si^{2+}(3s^2)^1S + He^{+}(1s)^2S \quad (2)$$

$$Si^{4+}(2p^6)^1S + He(1s^2)^1S \rightarrow Si^{3+}(3l)^2L + He^{+}(1s)^2S \quad (3)$$

as well as electron capture by metastable ions

$$Si^{3+}(3s)^2S + He(1s^2)^1S \rightarrow Si^{2+}(3s3p)^{1,3}P^0 + He^{+}(1s)^2S \quad (4)$$

$$Si^{3+}(3p)^2P^0 + He(1s^2)^1S \rightarrow Si^{2+}(3s3p)^{1,3}P + He^{+}(1s)^2S \quad (5)$$

$$\rightarrow Si^{2+}(3s^2)^1S + He^{+}(1s)^2S. \quad (6)$$

Here we report a complete ab initio molecular treatment of the Si^{2+} + H, Si^{3+} + He and Si^{4+} + He charge-transfer processes and compare them to other theoretical and experimental approaches, in particular the very recent work of Stancil and coworkers [9, 15] and Clarke and coworkers [10, 14], in order to provide an interpretation of the mechanism of such processes.

2 Computational method

2.1 Adiabatic potential-energy curves

The potential-energy curves were determined for a large number of interatomic distances in the 2–30 au range by means of multiconfiguration self-consistent field calculations followed by configuration interaction based on the CIPSI = configuration interaction by perturbation of a multiconfiguration wavefunction selected interactively (CIPSI) algorithm [18, 19]. A nonlocal pseudopotential [20] was used to represent the core electrons of the silicon atom. Special care was taken to construct sets of determinants providing the same level of accuracy over the whole distance range with a threshold of $\eta = 0.001$ for the perturbation contribution providing a good description of the wavefunctions.

The basis of atomic functions used to represent the silicon ions was a $9s7p2d$ basis of Gaussian functions contracted to $5s4p2d$, optimized on $Si^{3+}(3s)^2S$ and $Si^{2+}(3s3p)^2P$ from the basis sets of McLean and Chandler [21]. This basis set provides overall good agreement with experimental data [22] for a large number of silicon levels in an energy range of about 100 eV (Table 1). For helium and hydrogen, we took, respectively, the $4s1p$ and $5s3p$ basis already used in previous applications [23, 24]. This basis of atomic functions may be compared to the larger coupled-cluster polarized valence triple zeta and augmented coupled-cluster polarized valence quadruple zeta basis sets of Woon and Dunning [25] with errors of the order of 10^{-4} au on the Hartree–Fock energies.

2.2 Coupling matrix elements

The radial coupling matrix elements between all pairs of states of the same symmetry were calculated by means of the finite-difference technique:

$$g_{KL}(R) = \langle \Psi_K \ \mathrm{d}/\mathrm{d}R \ \Psi_L \rangle = \lim_{\Delta \rightarrow 0} 1/\Delta \langle \Psi_K(R) \ \Psi_L(R+\Delta) \rangle \ ,$$

Table 1. Comparison of the calculated atomic levels with the experimental data of Bashkin and Stoner (eV)

Levels	Calculation	Experiment
$Si^{4+}(2p^6)^1S$	44.881	45.140
$Si^{3+}(3p)^2P$	8.781	8.876
$Si^{3+}(3s)^2S$	0.0	0.0
$Si^{2+}(3p^2)^3P$	−17.295	−17.378
$Si^{2+}(3s3d)^1D$	−18.125	−18.339
$Si^{2+}(3p^2)^1D$	−18.119	−18.339
$Si^{2+}(3s3p)^1P$	−22.751	−23.215
$Si^{2+}(3s3p)^3P$	−26.799	−26.923
$Si^{2+}(3s^2)^1S$	−33.191	−33.491
$Si^{+}(3s)^2S$	−49.356	−49.831

with the parameter $\Delta = 0.0012$ au as previously tested and using the silicon nucleus as the origin of the electronic coordinates. For reasons of numerical accuracy, we performed a three-point numerical differentiation using calculations at $R + \Delta$ and $R - \Delta$ for a very large number of interatomic distances in the avoided-crossing region.

The rotational coupling matrix elements $\langle \Psi_K \, iL_y \, \Psi_L \rangle$ between Σ–Π molecular states were determined directly from the quadrupole moment tensor, which allows the consideration of translation effects in the collision dynamics. In the approximation of the common translation factor [26], the radial and rotational coupling matrix elements between states Ψ_K and Ψ_L may indeed be transformed, respectively, into

$$\langle \Psi_K \, \mathrm{d}/\mathrm{d}R - (\varepsilon_K - \varepsilon_L) z^2/2R \, \Psi_L \rangle,$$
$$\langle \Psi_K \, iL_y + (\varepsilon_K - \varepsilon_L) zx \, \Psi_L \rangle \ ,$$

where ε_K and ε_L are the electronic energies of states Ψ_K and Ψ_L and z^2 and zx are the components of the quadrupole moment tensor. This expression, valid for any choice of electronic coordinates, was used with the silicon nucleus as the origin of the electronic coordinates.

2.3 Collision dynamics

The collision dynamics was treated in the electron volt energy range by a semiclassical approach using the EIKONXS program [27] based on an efficient propagation method in the case of the Si^{2+} + H and Si^{4+} + He reactions. Both radial and rotational coupling matrix elements were taken into account, as well as translation effects, although they are expected to be low at these energies, by introducing common translation factors as proposed by Errea et al. [26]. For the Si^{3+} + He collision system, a quantum mechanical approach was preferred. Allowance for translation effects was made by introducing appropriate reaction coordinates [28, 29], which led to a modification of the radial and rotational matrix elements similar in form to those resulting from application of the common translation factor method [26]. Subsequently, adiabatic transformation of the molecular data is first carried out before solving the coupled differential equations for the determination of the **S** matrix. The rate coefficients, $k(T)$, were calculated by averaging the cross sections over a Maxwellian velocity distribution at temperature T.

3 The $Si^{2+}(3s^2)$ + H system

As far as only the ground-state is concerned, this is a relatively simple system for which only three states have to be taken into account: the entry channel correlated to $^2\Sigma^+[Si^{2+}(3s^2)^1S + H(1s)^2S]$ and the $^2\Sigma^+$ and $^2\Pi$ states correlated to the one-electron capture channel $[Si^+(3s^23p)^2P + H^+]$. The potential-energy curves are displayed in Fig. 1. In accordance with previous work

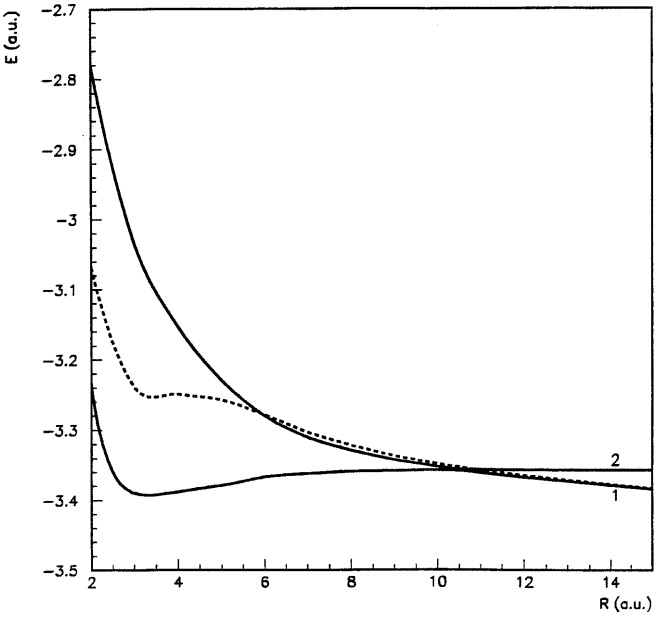

Fig. 1. Adiabatic potential-energy curves for the $^2\Sigma^+$ and $^2\Pi$ states of SiH^{2+}: $^2\Sigma$ (——); $^2\Pi$ (- - - - -). *1*: Σ, Π states dissociating to $[Si^+(3s^23p)^2P + H^+]$; *2*: Σ state dissociating to $[Si^{2+}(3s^2)^1S + H(1s)]$

Table 2. Position, energy gap and height of the radial coupling matrix element at the crossing point for the $^2\Sigma^+$ states of SiH^{2+}

Molecular states	R_x (au)	ΔU_x (eV)	g_{ij} (au)	Reference
$Si^{2+}(^1S)$–$Si^+(^2P)$	9.93	0.131	–	3
	9.75	0.080	1.56	4
	10.4	0.052	2.35	10
	10.5	0.046	2.47	This work

[2–4, 10] (Table 2), the potentials show a sharp avoided-crossing at $R = 10.5$ au between the entry channel and the $^2\Sigma^+$ one-electron capture level corresponding to a sharp peak, 2.47 au high, of the radial coupling matrix element. A deep potential well for the $X^2\Sigma^+$ ground-state of the SiH^{2+} diatomic may be observed with a barrier of 1.04 eV, in quite good agreement with the calculations of Koch et al. [30]. Generally speaking, our calculated spectroscopic quantities compare positively with the most recent values obtained for SiH^{2+} [30–34] (Table 3).

The collision dynamics was performed in the 0.002–0.1 au velocity range and was compared to the ab initio results of Clarke et al. [10] with radial coupling only, as well as with the quantal close-coupling approach of Gargaud et al. [4] using model potentials and the Landau–Zener analysis of Bates and Moiseiwitsch [1]. The corresponding rate coefficients are presented in Fig. 2. Globally speaking, the results obtained for the capture from the ground-state Si^{2+} ion are in relative agreement. As already noted by Clarke et al. [10], the results of their quantal close-coupling approach differs slightly from the results of Gargaud et al. [4]. and Bates and Moiseiwitsch [1]. They are, in contrast, in good agreement with ours for high temperatures, with the use of a semiclassical

Table 3. Spectroscopic constants (cm^{-1}) for the ground $X^2\Sigma^+$ state of SiH^{2+}

Calculation	R_e (au)	ω_e	$\omega_e\chi_e$	B_e	α_e	D_e (eV)	Barrier (eV)
This work	3.29	1037.0	9.2	5.711	0.558	−1.45	1.04
H^v [31]	3.20	1142.7	9.6	6.08	0.486	−1.47	1.12
MP4 [30]	3.10	1121				−1.54	0.89
CASSCF [29]	3.30	958.0	10.3	5.685		−1.41	1.06
MRD-CI [29]	3.30	965.2	8.7	5.685		−1.43	1.07
MOLPRO [33]	3.29	965					1.19

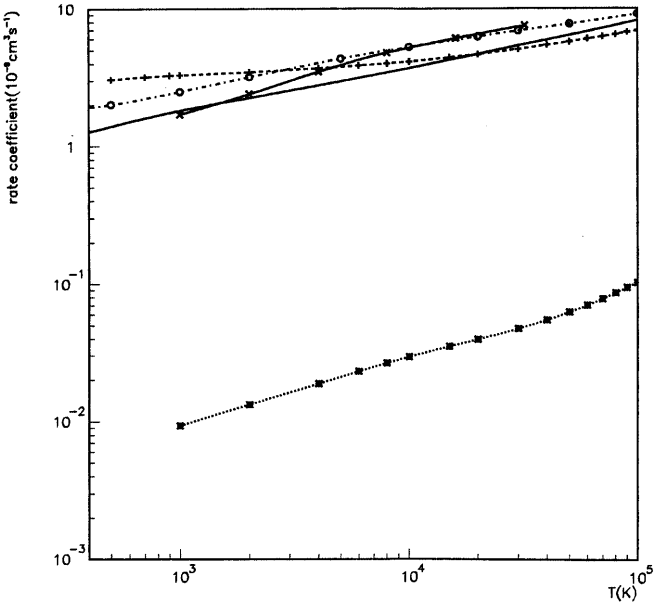

Fig. 2. Rate coefficients (10^{-9} cm^3 s^{-1}) for charge-transfer recombination of Si^{2+} ions from H. This work (————); Clarke et al. [10] (-+-+-+-); Gargaud et al. [4]; (-·○·○·-); Bates and Moiseiwitsch [1] (— × — ×); capture from $Si^{2+}(3s3p)$ [10] (···*···*)

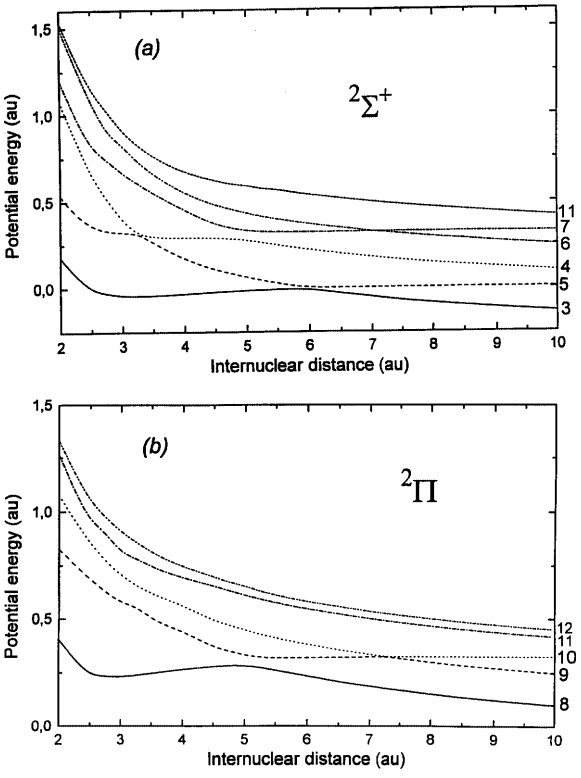

Fig. 3a, b. Adiabatic potential-energy curves for the $^2\Sigma^+$ and $^2\Pi$ states of $SiHe^{3+}$. *3*: Σ state dissociating to $[Si^{2+}(3s^2)^1S + He^+(1s)^2S]$; *4*: Σ state dissociating to $[Si^{2+}(3s3p)^3P + He^+(1s)^2S]$; *5*: Σ state dissociating to $[Si^{3+}(3s)^2S + He(1s^2)^1S]$; *6*: Σ state dissociating to $[Si^{2+}(3s3p)^1P + He^+(1s)^2S]$; *7*: Σ state dissociating to $[Si^{3+}(3p)^2P + He(1s^2)^1S]$; *8*: Π state dissociating to $[Si^{2+}(3s3p)^3P + He^+(1s)^2S]$; *9*: Π state dissociating to $[Si^{2+}(3s3p)^1P + He^+(1s)^2S]$; *10*: Π state dissociating to $[Si^{3+}(3p)^2P + He(1s^2)^1S]$; *11*: Σ and Π states dissociating to $[Si^{2+}(3p^2)^1D + He^+(1s)^2S]$; *12*: Σ and Π states dissociating to $[Si^{2+}(3s3d)^1D + He^+(1s)^2S]$

approach in our calculation leading to some discrepancies for lower temperatures. This agreement may be directly correlated to the position and energy separation at the crossing point (Table 2), which are in excellent agreement in both ab initio approaches. It is worth noting the rate coefficients corresponding to the electron capture process from the $Si^{2+}(3s3p)^3P^0$ metastable state

$$Si^{2+}(3s3p)^3P^0 + H(1s)^2S \rightarrow Si^+(3s3p^2)^2D + H^+ \quad (7)$$

$$\rightarrow Si^+(3s^23p)^2P^0 + H^+ \quad (8)$$

which has been determined by Clarke et al. [10] to be about 2 orders of magnitude lower than the capture by the ground-state ion.

4 The Si^{3+} + He system

For this system, the charge-transfer process from both ground-state $Si^{3+}(3s)$ and metastable $Si^{3+}(3p)$ ions were investigated. The potential-energy curves are displayed in Fig. 3. These results may be compared to the SCVB = spin coupled valence bond (SCVB) calculations of Clarke and coworkers [14, 15] and to the empirical potentials of Butler and Dalgarno [3] (Table 4). They show close agreement, especially for the energy gaps at the crossing points, but some uncertainties remain about the position of the avoided crossings and, even though the radial couplings are similar in shape in both ab initio calculations, the maximum peak values are lower in our work than in the SCVB approach.

The coupling equations were solved simultaneously for all the levels involved in the charge-transfer process from both the ground-state and the excited entry channels. The calculated rate coefficients are displayed in Fig. 4 and are compared to the ion-trap experiment of Fang and Kwong [16]. For the capture process from the ground-state $Si^{3+}(3s)$ ion, global agreement is observed between the Landau–Zener calculations of Butler and

Table 4. Position, energy gap and height of the radial coupling matrix element at the crossing point for the $^2\Sigma^+$ states of $SiHe^{3+}$

Molecular states	R_x (au)	ΔU_x (eV)	g_{ij} (au)	Reference
$Si^{3+}(^2S)$–$Si^{2+}(^3P)$	3.2	0.707	1.6	This work
	3.4	0.795	4.0	15
$Si^{2+}(^3P)$–$Si^{2+}(^1P)$	4.9	1.570	0.73	This work
	5.0	1.525	1.0	15
$Si^{3+}(^2S)$–$Si^{2+}(^1S)$	6.1	0.282	–	3
	6.0	0.250	1.76	This work
	6.3	0.270	2.7	15
$Si^{3+}(^2P)$–$Si^{2+}(^1P)$	7.0	0.054	4.54	This work
	7.3	0.051	7.7	15

Dalgarno [3] and the ab initio treatments [13, 15]. In particular, even though the results of Stancil et al. [15] are in magnitude higher than ours, both quantum mechanical approaches show almost the same shape with a decrease in the rate coefficients with temperature and an inflection towards lower temperatures. Nevertheless, although some uncertainty, in particular in the determination of the temperature in the trap, should be taken into account, all theoretical methods provide rate coefficients lower than the experimental point of Fang and Kwong [16]. In contrast, our calculated rate coefficients for capture from the metastable $Si^{3+}(3p)$ are of the same magnitude as those from the ion-trap experiment [16]. From the hypothesis of the presence of excited $Si^{3+}(3p)$ ions in the experiment, we would then have a fair agreement between experimental and theoretical results. In the ion-trap experiment, Si^{3+} ions are produced by laser ablation and can then be in a variety of excited electronic states immediately after their production, but, according to Fang and Kwong [16], all the stored Si^{3+} ions are expected to be in their ground-state, as measurements are performed 0.4 s after the ions have been produced and trapped. This assumption could be tested efficiently by measurements at different temperatures, as the rate coefficients for the capture from the ground-state $Si^{3+}(3s)$ ion are shown to exhibit quite different behaviour than those calculated in the process involving the excited $Si^{3+}(3p)$ ion, which remain almost constant with temperature.

5 The Si^{4+} + He system

The charge-transfer recombination from the $^1\Sigma^+$ $[Si^{4+} + He(1s^2)^1S]$ entry channel may lead to two exit channels correlated to the $^1\Sigma^+$ and $^1\Pi$ $[Si^{3+}(3p)^2P + He^+(1s)^2S]$ and $^1\Sigma^+$ $[Si^{3+}(3s)^2S + He^+(1s)^2S]$ levels. The potential-energy curves are displayed in Fig. 5. The $^1\Sigma^+$ potentials show two main avoided crossings: a very sharp one at $R = 6.95$ au between the entry channel and the $^1\Sigma^+$ $[Si^{3+}(3p)^2P + He^+(1s)^2S]$ level and an inner one at $R = 4.45$ au with the $^1\Sigma^+$ $[Si^{3+}(3s)^2S + He^+(1s)^2S]$ exit channel. The position and energy difference at the crossing points are

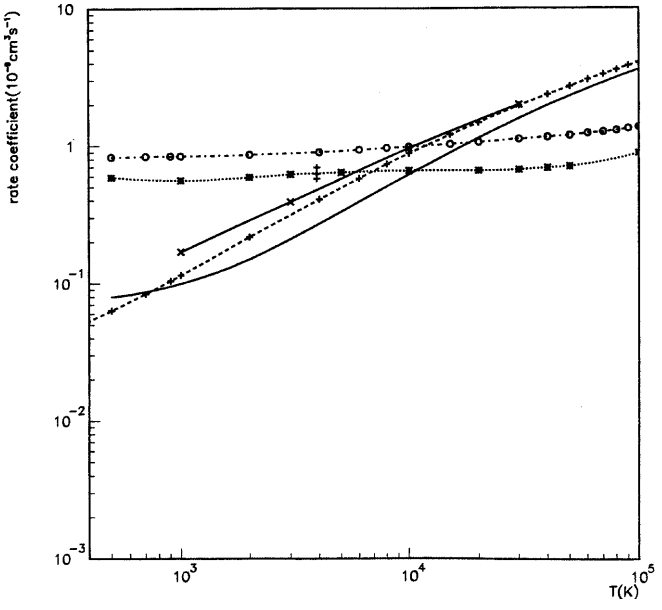

Fig. 4. Rate coefficients (10^{-9} cm^3 s^{-1}) for charge-transfer recombination of Si^{3+} ions from He. This work (——); Stancil et al. [15] (-+-+-+-); Butler and Dalgarno [3] (— × — ×); capture from $Si^{3+}(3p)$, this work (···*···*); capture from $Si^{3+}(3p)$, [15] (-·o-·o-·); experimental point, Fang and Kwong [16] (+)

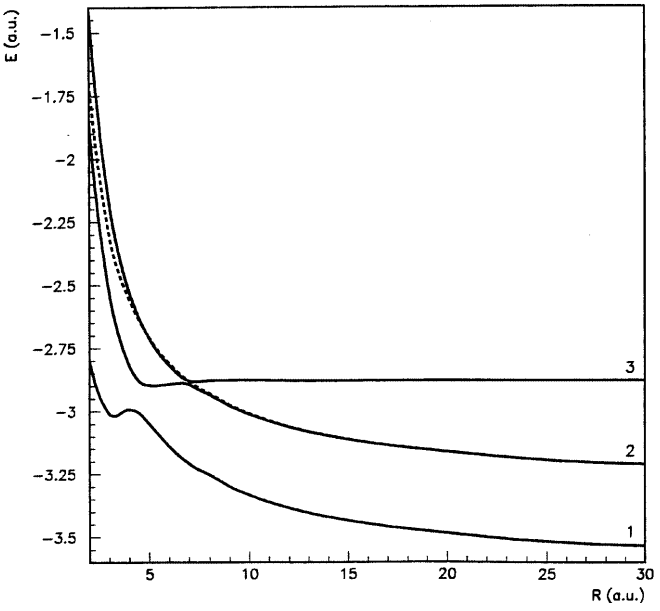

Fig. 5. Adiabatic potential-energy curves for the $^1\Sigma^+$ and $^1\Pi$ states of $SiHe^{4+}$: $^1\Sigma$ (——); $^1\Pi$ (-------). *1*: Σ state dissociating to $[Si^{3+}(3s)^2S + He^+(1s)^2S]$; *2*: Σ, Π states dissociating to $[Si^{3+}(3p)^2P + He^+(1s)^2S]$; *3*: Σ state dissociating to $[Si^{4+} + He(1s^2)]$

Table 5. Position, energy gap and height of the radial coupling matrix element at the crossing point for the $^1\Sigma^+$ states of $SiHe^{4+}$

Molecular states	R_x (au)	ΔU_x (eV)	g_{ij} (au)	Reference
$Si^{3+}(^2S)$–$Si^{3+}(^2P)$	4.0	2.1	–	3
	4.5	2.46	–	5
	4.6	3.385	0.8	9
	4.45	3.417	0.74	This work
$Si^{4+}(^1S)$–$Si^{3+}(^2P)$	7.0	0.112	–	3
	6.975	0.244	–	5
	7.0	0.344	2.4	9
	6.95	0.365	2.38	This work

presented in Table 5 and are compared to the empirical potentials of Butler and Dalgarno [3]. Although the positions of the avoided crossings are in close agreement, the energy gaps are significantly different for the empirical and model potential approaches compared to the SCVB and CIPSI methods, showing the necessity for an ab initio treatment for such a system.

The collision dynamics was performed in the 0.002–0.1 au velocity range and rate coefficients are compared to the Landau–Zener results of Butler and Dalgarno [3] and the quantal close-coupling approach taking account only of the radial coupling of Stancil et al. [9] (Fig. 6). While the rate coefficients obtained by a Landau–Zener approach are nearly constant with temperature, the model potential and the ab initio treatments show a relatively strong increase with increasing temperature. The results, in particular those of the two ab initio approaches, are in fair agreement for high temperatures, with some discrepancies appearing for lower ones, partly due to the use of a semiclassical approach in our calculation, but the discrepancy between the ab initio and model potential methods should be correlated to the differences shown by molecular structure calculations. All these theoretical approaches are, however, in complete disagreement, by 2 orders of magnitude, with the ion-trap experimental data of Fang and Kwong [17], at least for the charge-transfer process from the $Si^{4+}(2p^6)$ ion. According to the discussions previously developed for Si^{2+} + H and Si^{3+} + He, the experimental point might possibly correspond to the capture from an excited Si^{4+} ion, which could perhaps explain the difference of 2 orders of magnitude for the rate coefficients, as shown for Si^{2+} + H, but the only candidate, $Si^{4+}(2p^5 3s)$, seems quite improbable as it is very high in energy compared to the ground-state $Si^{4+}(2p^6)$ ion. Such assumptions need to be tested by further calculations and experiments at different temperatures.

6 Concluding remarks

This work provides accurate ab initio potential-energy curves and coupling matrix elements for the Si^{2+} + H, Si^{3+} + He and Si^{4+} + He collisional systems. Both radial and rotational couplings have been taken into account in a fair description of the charge-transfer recombination process including translation effects which remain weak over the whole collision energy range. Good agreement between the theoretical approaches is observed, but the comparison with the ion-trap experiments of Fang and Kwong [16, 17] might necessitate the consideration of excited-state ions. Such an assumption has to be tested by calculations on charge-transfer processes from metastable states and by further experiments providing the variation of the rate coefficients with temperature.

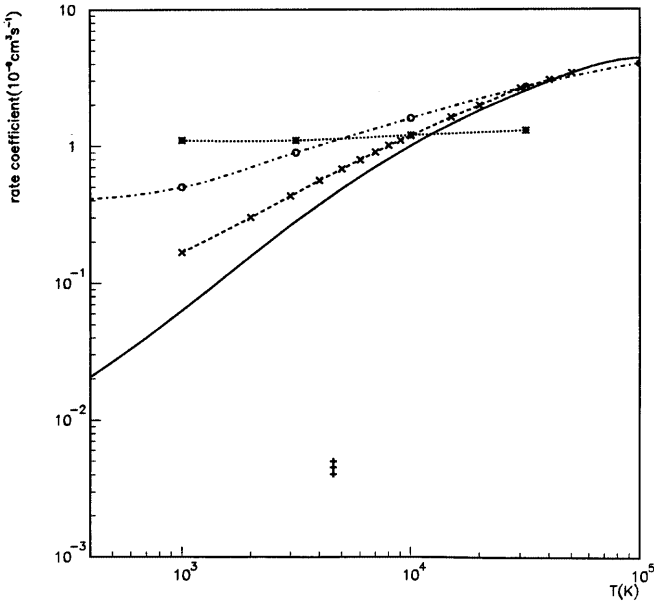

Fig. 6. Rate coefficients (10^{-9} cm^3 s^{-1}) for charge-transfer recombination of Si^{4+} ions from He. This work (——); Stancil et al. [9] (-x-x-x); Opradolce et al. [5] (··○··○··); Butler and Dalgarno [3] (···*···*); experimental point, Fang and Kwong [17] (+)

References

1. Bates DR, Moiseiwitsch BL (1954) Proc Phys Soc A 67: 805
2. McCarroll R, Valiron P (1976) Astron Astrophys 53: 83
3. Butler SE, Dalgarno A (1980) Astrophys J 241: 838
4. Gargaud M, McCarroll R, Valiron P (1982) Astron Astropys 106: 197
5. Opradolce L, McCarroll R, Valiron P (1985) Astron Astrophys 148: 229
6. Gargaud M, McCarroll R (1988) J Phys B 21: 513
7. Pieksma M, Gargaud M, McCarroll R, Havener CC (1996) Phys Rev A 54: R13
8. Herrero B, Cooper IL, Dickinson AS (1996) J Phys B 29: 5583
9. Stancil PC, Zygelman B, Clarke NJ, Cooper DL (1997) Phys Rev A 55: 1064
10. Clarke NJ, Stancil PC, Zygelman B, Cooper DL (1998) J Phys B 31: 533
11. Bacchus-Montabonel MC, Ceyzeriat P (1998) Phys Rev A 58: 1162
12. Bacchus-Montabonel MC (1998) Chem Phys 237: 245
13. Honvault P, Bacchus-Montabonel MC, Gargaud M, McCarroll R (1998) Chem Phys 238: 401
14. Clarke NJ, Cooper DL (1998) J Chem Soc Faraday Trans 94: 3295
15. Stancil PC, Clarke NJ, Zygelman B, Cooper DL (1999) J Phys B 32: 1523
16. Fang Z, Kwong VHS (1997) Astrophys J 483: 527
17. Fang Z, Kwong VHS (1999) Phys Rev A 59: 342
18. Huron B, Malrieu JP, Rancurel P (1973) J Chem Phys 58: 5745

19. Evangelisti S, Daudey JP, Malrieu JP (1983) J Chem Phys 75: 91
20. Pélissier M, Komiha N, Daudey JP (1988) J Comput Chem 9: 298
21. McLean AD, Chandler GS (1980) J Chem Phys 72: 5639
22. Bashkin S, Stoner JO (1975) Atomic energy levels and grotrian diagrams. North Holland, Amsterdam
23. Bacchus-Montabonel MC (1992) Phys Rev A 46: 217
24. Bacchus-Montabonel MC, Fraija F (1994) Phys Rev A 49: 5108
25. Woon DE, Dunning TH Jr (1993) J Chem Phys 98: 1358
26. Errea LF, Mendez L, Riera A (1982) J Phys B 15: 101
27. Allan RJ, Courbin C, Salas P, Wahnon P (1990) J Phys B 23: L461
28. Gargaud M, McCarroll R, Valiron P (1987) J Phys B 20: 1555
29. McCarroll R, Crothers DSF (1994) Bates DR, Bederson B (eds) Advances in atomic, molecular and optical physics, vol 23. Academic New York, p 253
30. Koch W, Frenking G, Chang CC (1986) J Chem Phys 84: 2703
31. Koch W, Frenking G, Schwarz H, Maquin F, Stahl D (1986) J Chem Soc Perkin Trans II 757
32. Park JK, Sun H (1993) J Chem Phys 99: 1844
33. Nefedova VV, Boldyrev AI, Simons J (1995) Int J Quantum Chem 55: 441
34. Chambaud G, Bliman S, Rosmus P, Senekowitsch J, O'Neil S (1995) Nucl Instrum Methods Phys Res Sect B 98: 208